Modeling Photonic Molecules Using Graph Theory

Student: Gabriel Rezende da Ascenção
Electrical engineering Department - DEE
Federal University of São Carlos - UFSCar
São Carlos, SP
http://lattes.cnpq.br/9822738140422204

Advisor: Luis Alberto Mijam Barêa
Electrical engineering Department - DEE
Federal University of São Carlos - UFSCar
São Carlos, SP
http://lattes.cnpq.br/7929868663210908

***Resumo*—This work aims to demonstrate a practical way to model Photonic Molecules (PMs), using tools often used in control theory. It is shown here how it is possible to model systems composed of coupled electromagnetic resonators using a graph representation. Furthermore, it is shown the application of this modeling method for different photonic systems and how the response predicted by this method does agree with the response expected by the coupled oscillators theory, and how this tool predicts the transition between dark states and quasi-dark states when the system's symmetry is broken.**

***Index Terms*—Photonic Molecules, Dynamical Systems, Coupled Oscillators, Microcavities, Graph Theory.**

I. Introduction

Integrated photonics has experienced essential developments in the past few decades. In addition to showing itself as a candidate tool to solve the problem of the increasing data demand, research on integrated photonics has introduced remarkable advances in areas such as biosensing [1], [2], on-chip optomechanics [3], [4], and on-chip quantum computing [5], [6].

Many applications of integrated photonics are based on fundamental construct blocks, in which micro resonators ring-shaped or disk-shaped are widely present, being almost ubiquitous.

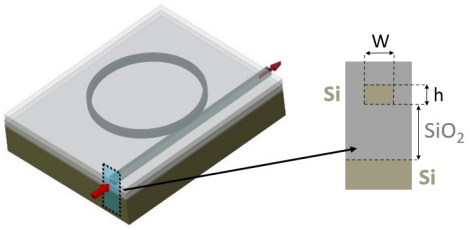

Fig. 1. **Example of a ring resonator coupled to a waveguide. This example shows a device constructed over an SOI platform (Silicon Over Insulator), in which the width and the height of the waveguides are represented by W and h, respectively. From:** BAREA [7].

Figure 1 shows an example of one of these ring resonators coupled to a bus waveguide, this figure also shows an example of the construction of these devices over platform silicon over insulator (SOI) one of the most important platforms for photonics. In a device like this, the input wave travels through the bus waveguide until it reaches the coupling region between the optical oscillator (microring resonator) and the bus waveguide. Currently, one portion of the light continues traveling through the bus waveguide while the other portion is coupled to the resonator. After one turn over the resonator, the wave will experience interference over itself. This interference will be constructive if the length of the resonator is an integer multiple of the wave's wavelength. In this case, there will also be a destructive interference between the light coming out from the resonator which is re-coupling to the bus waveguide. In such a situation (resonant case) there is no output power at the end of the bus waveguide, and therefore the wave is completely confined within the resonator.

Although these components can store light in small volumes, being able to generate high-Q resonances, when they are used alone their performance is limited due to their intrinsic dependence between the cavity's radius (R), free spectral range (FSR), and the Q factor. [7]. The dependence between the radius of the cavity and the FSR (the interval between two consecutive resonances) is explicit and comes from the constructive interference condition. This means that the larger the cavity's length the smaller the FSR, as is shown in equation 1.

$$FSR = \frac{\lambda^2}{nL} \tag{1}$$

In the equation 1, n is the refractive index of the cavity and L represents the cavity's length, λ is the wavelength of the resonant wave.

The Q factor dependence on the cavity's radius comes from the intrinsic loss mechanisms of the cavity, in which the dominant effect is the light scattering in the cavity's edges due to its roughness. This means that a bigger radius implies higher Q factors, which is a limiting relation in applications where the area of these devices is critical, as indeed is in integrated applications on chips. The equation 2 shows the dependence between the Q factor and the length of the device.

$$Q = \frac{nL}{\lambda}\frac{FSR}{FWHM} = \frac{\lambda}{FWHM} \tag{2}$$

On the equation 2 $FWHM$ is the full width at half maximum of the resonances.

Figure 2 shows an example of the intrinsic dependencies discussed above.

By looking at Figure 2 it is possible to see when the cavity has a bigger radius the resonances appear sharper i.e

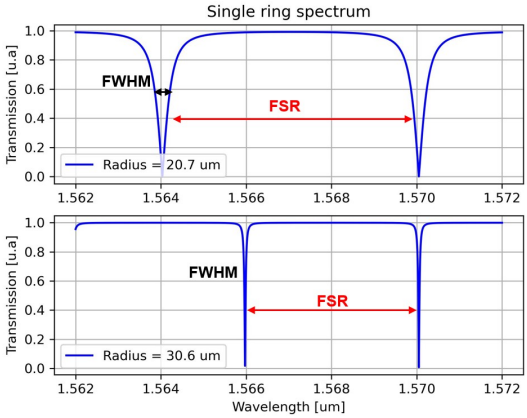

Fig. 2. **Illustrative example of two spectral responses from cavities with different radii. From:** Author

the FWHM is reduced, which is a consequence of higher Q factors, on the other hand, the FSR was reduced.

To overcome this problem, researchers have proposed the use of coupled resonators instead of one single cavity, which was called Photonic Molecules (PMs). The use of PMs in photonic systems gives the system more degrees of freedom. This versatility allows one to do spectral engineering over the system, manipulating its degrees of freedom to obtain spectral responses impossible to get with one single oscillator [7], which has led the use of photonic resonators to new applications [2], [8], [9]. Figure 3 shows two examples of PMs formed by coupled resonators embedded in a main microring resonator which is coupled to a bus waveguide.

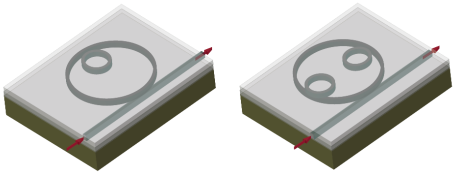

Fig. 3. **Examples of coupled resonators. From:** BAREA [7].

On the other hand, this method of coupling cavities inside or outside a main ring allows the observation of new effects that depend on the position of the coupled cavities, such as the emergence of dark states and quasi-dark states [10]. Therefore, correctly describing the behavior of these devices is very important for research in this field of knowledge as well as taking advantage of the best spectral engineering allowed by these PMs. For this reason, in this work, it will be shown how it is possible to model such PMs using graph theory, a mathematical tool that proves to be exceptionally practical for this application. Furthermore, the formulation shown here may help future students or researchers to start their work with these compact building blocks for integrated photonics.

II. Metodology

A. Current main tools

Nowadays, most of the articles in the literature present the modeling of systems composed of microring resonators using two distinct methods: Transfer Matrix Method (TMM) [11] and Coupled Mode Theory (CMT) [12]. The CMT is a perturbative method, based on the formalism of coupled oscillators, widely studied in classical physics. As a perturbative formalism, its predictions are restricted to weakly coupled systems with low losses [10].

A general formulation of CMT is shown in [13]. Using this formulation, a photonic system's dynamical and stationary response can be found starting from a system of first order differential equations. For a system composed of the same number of ports and optical oscillators, these equations are shown on 3 and 4.

$$\frac{d\vec{a}}{dt} = (j\Omega - \Gamma) \cdot \vec{a} + I \cdot K \cdot \vec{S_{in}} \tag{3}$$

$$\vec{S_{out}} = \vec{S_{in}} + K \cdot \vec{a} \tag{4}$$

On equations 3 and 4, $\vec{a}$ represents the amplitude of the optical mode in each oscillator, so if the system is composed of N resonators, $\vec{a}$ will have N components. The matrix $\Omega_{N\times N}$ represents the resonant frequencies of the bare system in its diagonal terms, while the off-diagonal terms represent the coupling between the oscillation modes. The system's losses are accounted for in the $\Gamma_{N\times N}$ matrix, which represents both intrinsic losses and the decay due to the coupling. $\vec{S_{in}}$ and $\vec{S_{out}}$ represent the N input and output ports of the system. K is the coupling vector representing the coupling between the input/output waves and the system's modes. Thus obtaining the response of a PM is very straight with the CMT formalism, and it is done just by solving a first-order ordinary differential equation (ODE) system. This formalism also has the advantage that it allows one to obtain the normal modes of the system using linear algebra techniques over the Ω matrix. The eigenfrequencies are the eigenvalues of Ω while the eigenvectors represent the system's resonant modes. Although this formalism provides a simple formulation for coupled-resonators systems, it has some limitations, for example on the prediction of quasi-dark-states, as shown in [10].

TMM, on the other hand, is a formalism based on the combined interference of light coming from the multiple optical paths allowed in a photonic system [10]. To model PMs using this tool it is necessary to account for the waves' phase shift and decay when passing through the system's elements (which can be bus waveguides or microring resonators). That can be done using the following equation:

$$S_{out} = e^{(j\omega-\alpha)T} = Ae^{j\omega T} \tag{5}$$

In the equation 5, the decay term $e^{-\alpha T}$ was represented in a compact notation by the coefficient A. ω is the angular frequency of the light and T represents the time taken by the light to travel over an element, and it is given by the equation:

$$T = \frac{Ln_{eff}}{c} \tag{6}$$

L and n_{eff} are respectively the length and the effective refraction index of the element, and c is the speed of light at vacuum.

The coupling between the elements is modeled using the transfer matrices equations, which are represented by equations 7 and 8. These equations represent the coupling between two and three parallel bus waveguides, respectively.

$$\begin{bmatrix} E_2 \\ E_4 \end{bmatrix} = \begin{bmatrix} t & jk \\ jk & t \end{bmatrix} \cdot \begin{bmatrix} E_1 \\ E_3 \end{bmatrix} \tag{7}$$

$$\begin{bmatrix} E_8 \\ E_6 \\ E_{10} \end{bmatrix} = \begin{bmatrix} \frac{t+1}{2} & \frac{-jk}{\sqrt{2}} & \frac{t-1}{2} \\ \frac{-jk}{\sqrt{2}} & t & \frac{-jk}{\sqrt{2}} \\ \frac{t-1}{2} & \frac{-jk}{\sqrt{2}} & \frac{t+1}{2} \end{bmatrix} \cdot \begin{bmatrix} E_7 \\ E_5 \\ E_9 \end{bmatrix} \tag{8}$$

The vectors present in equations 7 and 8 represent, particularly, the coupling ports of the device shown in figure 4. In this figure, E_1 is the input port of the PM, and E_2 is the output port. The full device is composed of three race-track-shaped resonators. This shape allows better control of the coupling, represented in equations 7 and 8 by the coupling coefficient k. It is important to notice that both transfer matrices are unitary, which guarantees that the input power is conserved, as a consequence, the equation $k^2 + t^2 = 1$ is satisfied, where t is called the transmission coefficient.

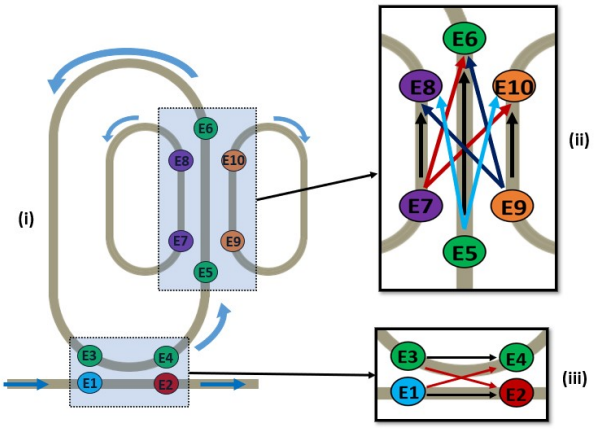

Fig. 4. **An illustrative example of a photonic molecule containing two different types of coupling (between two parallel waveguides and between three parallel waveguides). (i) shows the full picture of the device while (ii) and (iii) show the coupling regions in more detail. From:** Author

To obtain the relation between the output and the input ports of the system (i.e $\frac{E_2}{E_1}$) it is necessary to solve the matrix equations 7 and 8, considering the wave's propagation through the full device, which clearly demands cumbersome algebraic work, more complex than in the CMT method. However, the TMM formalism has the advantage of having no limitations on modes' predictions and it is not limited to weakly coupled with low losses systems [10]. Therefore, a way to apply the TMM formalism without such hard algebraic work is very suitable for modeling PMs, that is where the system's representation using directional graphs shows up as an easy and practical tool.

B. Graphs representation method

The graph representation method applied to resonators was introduced by Rezende [14]. In this method, due to the system's linearity, it is possible to represent the system as a block diagram or as an equivalent directional graph diagram, in which the system's ports are represented by vertices, and the relations between them are represented by the graph's edges. An example of a simple system's graph representation is illustrated in figure 5, for a single cavity coupled to a bus waveguide.

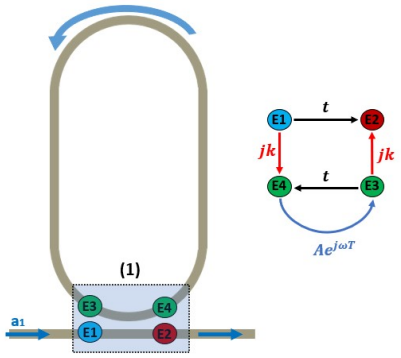

Fig. 5. **Single cavity coupled to a waveguide and its graph representation. The highlighted area (1) is the coupling region, where a_1 represents an incoming wave, E_1 and E_2 represent the input and output ports respectively. From:** Author

In the system presented in figure 5 both the coupling relations given by TMM, as well as the propagation terms are represented in the graph, which is the great advantage of the graph's representation. It includes all the relations in the system, allowing one to apply Mason's rule [15] to obtain the direct connection between any two arbitrary ports. Mason's rule is a tool often used in control systems to simplify block diagrams, i.e, obtain the equivalent relation (gain) of two arbitrary points in the diagram.

The most practical way to apply Mason's rule to the photonics systems shown in this work is to use it in its matrix form. To do this it is necessary to construct the adjacency matrix of the graphs, which shows how a given vertex described in column n depends on another vertex described in line m. For the system of figure 5 the adjacency matrix is shown in equation 9. In this representation, an element in the line m and column n represents the relation between the port E_n and E_m (the arrow pointing from E_m to E_n). This means for example that the element A_{14} is the relation between E_1 and E_4, which is jk as shown in equation 7 and by the arrow in the system of 5, connecting E_1 and E_4.

$$A_{4x4} = \begin{bmatrix} 0 & t & 0 & jk \\ 0 & 0 & 0 & 0 \\ 0 & jk & 0 & t \\ 0 & 0 & Ae^{j\omega T} & 0 \end{bmatrix} \tag{9}$$

As described in [15], the transfer function between the system's ports E_m and E_n is given by the element M_{mn} of the matrix M:

$$M = (I - A_{mxn})^{-1} \tag{10}$$

In the equation 10, I is the identity matrix. Performing the operations shown in equation 10, the matrix M is represented by:

$$M = \begin{bmatrix} 1 & \frac{t-Ae^{j\omega T}(k^2+t^2)}{1-Ate^{j\omega T}} & \frac{jkAe^{j\omega T}}{1-Ate^{j\omega T}} & \frac{jk}{1-Ate^{j\omega T}} \\ 0 & 1 & 0 & 0 \\ 0 & \frac{jk}{1-Ate^{j\omega T}} & \frac{1}{1-Ate^{j\omega T}} & \frac{t}{1-Ate^{j\omega T}} \\ 0 & \frac{jkAe^{j\omega T}}{1-Ate^{j\omega T}} & \frac{Ae^{j\omega T}}{1-Ate^{j\omega T}} & \frac{1}{1-Ate^{j\omega T}} \end{bmatrix} \tag{11}$$

For the system described here, the transfer function $\frac{E_2}{E_1}$ is desired, once it gives the relation between the output and the input of the system. Then, following Mason's rule, the element M_{12} of the matrix is taken. Considering the conservation of energy, given by $k^2 + t^2 = 1$, the transfer function between the input and output port is:

$$\frac{E_2}{E_1} = \frac{t - Ae^{j\omega T}}{1 - Ate^{j\omega T}} \tag{12}$$

The equation 12 is the same provided by pure TMM formalism, as can be found in [7], [11], [16]. The application of this method is easily done on more complex systems, as it is shown below, proving the advantage of its use to predict the spectral response of complex PMs.

Considering now a PM with two coupled resonators, as shown in figure 6 with its graph representation.

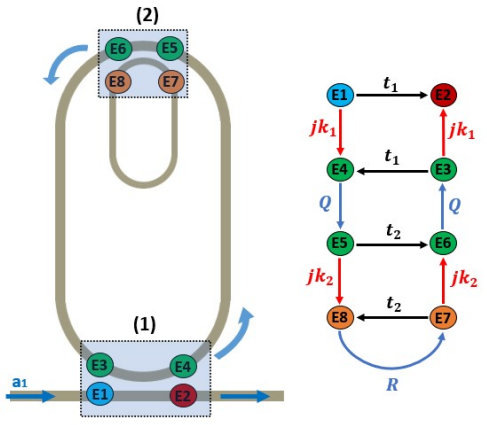

Fig. 6. **PM composed of two coupled resonators and its graph representation. The highlighted area (1) is the coupling region between the bigger cavity and the bus waveguide, while area (2) highlights the coupling region between the coupled cavities. From:** Author

In this device, there are two different coupling regions, and thus different coupling and transmission coefficients represented by k_1, k_2, t_1, and t_2. Furthermore, the two cavities also have different lengths, so the wave's phase shift and decay due to its propagation will not be the same for each resonator. These propagation effects are represented in the graph by Q, related to wave propagation in half of the larger cavity, and R, related to wave propagation along the smaller cavity. These parameters are given by:

$$Q = A_1^{\frac{1}{2}} e^{j\omega \frac{T_1}{2}} \tag{13}$$

$$R = A_2 e^{j\omega T_2} \tag{14}$$

In these equations, T_i and A_i represent the time taken by light to travel the entire cavity i and its decay after its propagation, respectively.

The adjacency matrix of this system is:

$$A = \begin{bmatrix} 0 & t_1 & 0 & jk_1 & 0 & 0 & 0 & 0 \\ 0 & 0 & 0 & 0 & 0 & 0 & 0 & 0 \\ 0 & jk_1 & 0 & t_1 & 0 & 0 & 0 & 0 \\ 0 & 0 & 0 & 0 & Q & 0 & 0 & 0 \\ 0 & 0 & 0 & 0 & 0 & t_2 & 0 & jk_2 \\ 0 & 0 & Q & 0 & 0 & 0 & 0 & 0 \\ 0 & 0 & 0 & 0 & 0 & jk_2 & 0 & t_2 \\ 0 & 0 & 0 & 0 & 0 & 0 & R & 0 \end{bmatrix} \tag{15}$$

Applying Mason's rule (equation 10) with the assistance of a symbolic computation software, as *Mathematica* or the *Sympy* package for python, on equation 15, the device's transfer function can be found. The equation 16 is the simplified transfer function of the device, obtained using the software *Mathematica*.

$$\frac{E_2}{E_1} = \frac{t_1 + Q^2(R - t_2) - Rt_1t_2}{1 + t_1Q^2(R - t_2) - Rt_2} \tag{16}$$

Another device with an interesting configuration is the one shown in figure 7. This device has three cavities with different lengths and coupling strengths (k_1, k_2, and k_3). The topology of this device is called serial because the wave does not couple on both smaller cavities at the same time, but sequentially.

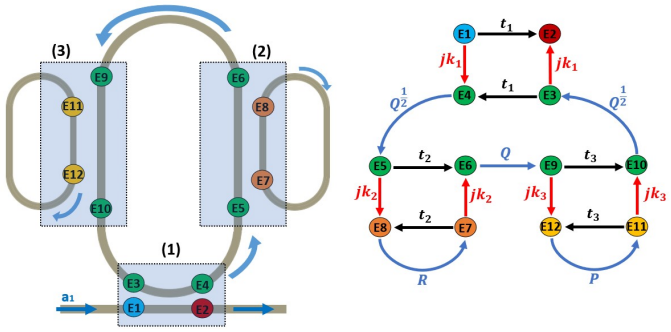

Fig. 7. **PM composed of three coupled resonators and its graph representation, the highlighted areas show the coupling regions. This topology is called serial. From:** Author

As can be seen in the graph of figure 7, this device has three propagation terms, each one for each resonator. While Q and R are the same terms shown in equations 13 and 14, and P is given by:

$$P = A_3 e^{j\omega T_3} \tag{17}$$

The adjacency matrix is twelve lines vs twelve columns matrix, represented in equation 18, which shows how it would be more cumbersome to model this device using just TMM's manual algebraic work.

$$\text{A} = \begin{bmatrix}
0 & t_1 & 0 & jk_1 & 0 & 0 & 0 & 0 & 0 & 0 & 0 & 0 \\
0 & 0 & 0 & 0 & 0 & 0 & 0 & 0 & 0 & 0 & 0 & 0 \\
0 & jk_1 & 0 & t_1 & 0 & 0 & 0 & 0 & 0 & 0 & 0 & 0 \\
0 & 0 & 0 & 0 & Q^{0.5} & 0 & 0 & 0 & 0 & 0 & 0 & 0 \\
0 & 0 & 0 & 0 & Q & t_2 & 0 & jk_2 & 0 & 0 & 0 & 0 \\
0 & 0 & 0 & 0 & 0 & 0 & 0 & 0 & Q & 0 & 0 & 0 \\
0 & 0 & 0 & 0 & Q & jk_2 & 0 & t_2 & 0 & 0 & 0 & 0 \\
0 & 0 & 0 & 0 & 0 & 0 & R & 0 & 0 & 0 & 0 & 0 \\
0 & 0 & 0 & 0 & 0 & 0 & 0 & 0 & 0 & t_3 & 0 & jk_3 \\
0 & 0 & Q^{0.5} & 0 & 0 & 0 & 0 & 0 & 0 & 0 & 0 & 0 \\
0 & 0 & 0 & 0 & 0 & 0 & 0 & 0 & 0 & jk_3 & 0 & t_3 \\
0 & 0 & 0 & 0 & 0 & 0 & 0 & 0 & 0 & 0 & P & 0
\end{bmatrix} \tag{18}$$

Applying the equation 10 over the equation 18, and taking the M_{12} term, with assistance of *Mathematica*, the following transfer function is obtained:

$$\frac{E_2}{E_1} = \frac{PQ^2(R-t_2) + t_1(R*t_2-1) + Q^2(t_2-R)t_3 + Pt_1(1-Rt_2)t_3}{Rt_2 + Qt_1(t_2-R)t_3 + P(Qt_1(R-t_2)+t_3-Rt_2t_3) - 1} \tag{19}$$

To simplify the equation 19 it is possible to consider that both smaller cavities have the same length and coupling strengths, which means that $P = R$ and $t_2 = t_3$. This simplification leads to:

$$\frac{E_2}{E_1} = \frac{Q^2(R-t_2)^2 - t_1(Rt_2-1)^2}{Q^2t_1(R-t_2)^2 - (Rt_2-1)^2} \tag{20}$$

The last device modeled in this work is shown in figure 8. This PM has two resonators arranged in parallel, and although the coupling between the three resonators is equal, they can have different lengths. Now, the coupling region (2) makes use of the equation 8. The adjacency matrix of this PM takes the form shown in equation 21.

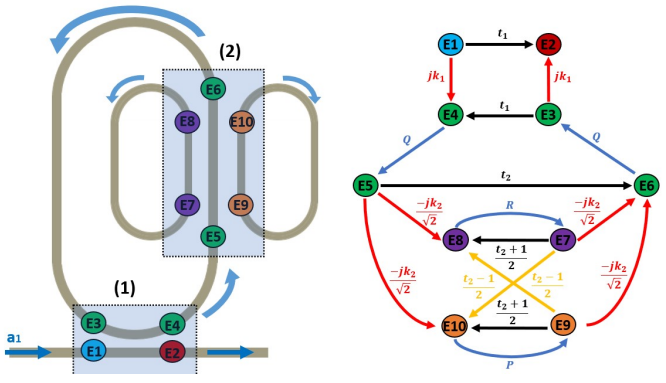

Fig. 8. **PM composed of three coupled resonators and its graph representation, the highlighted areas show the coupling regions, the region (1) is a simple coupling between two waveguides while the region (2) highlights the coupling between three parallel waveguides. This topology is called parallel. From:** Author

$$\text{A} = \begin{bmatrix}
0 & t_1 & 0 & jk_1 & 0 & 0 & 0 & 0 & 0 & 0 \\
0 & 0 & 0 & 0 & 0 & 0 & 0 & 0 & 0 & 0 \\
0 & jk_1 & 0 & t_1 & 0 & 0 & 0 & 0 & 0 & 0 \\
0 & 0 & 0 & 0 & Q & 0 & 0 & 0 & 0 & 0 \\
0 & 0 & 0 & 0 & 0 & t_2 & 0 & -j\frac{k_2}{\sqrt{2}} & 0 & -j\frac{k_2}{\sqrt{2}} \\
0 & 0 & Q & 0 & 0 & 0 & 0 & 0 & 0 & 0 \\
0 & 0 & 0 & 0 & 0 & -j\frac{k_2}{\sqrt{2}} & 0 & \frac{t_2+1}{2} & 0 & \frac{t_2-1}{2} \\
0 & 0 & 0 & 0 & 0 & 0 & R & 0 & 0 & 0 \\
0 & 0 & 0 & 0 & 0 & -j\frac{k_2}{\sqrt{2}} & 0 & \frac{t_2-1}{2} & 0 & \frac{t_2+1}{2} \\
0 & 0 & 0 & 0 & 0 & 0 & 0 & 0 & P & 0
\end{bmatrix} \tag{21}$$

On the equation 21, the terms P, Q, and R are the same propagation terms present in equations 17, 13, and 14.

Again, applying Mason's rule on equation 21, using the software *Mathematica*, the equation 22 is obtained as the device's transfer function.

$$\frac{E_2}{E_1} = \frac{PQ(1-2R+t_2)+Q(R+(R-2)t_2)-t_1(R+Rt_2-2)+Pt_1((2R-1)t_2)-1}{2-2Qt_1t_2+R(Qt_1-1)(1+t_2)+P(2Rt_2+Qt_1-1-t_2(1-2R+t_2))} \tag{22}$$

The above equation is very long and it can be simplified to the equation 23 if it is considered that both parallel cavities have the same length.

$$\frac{E_2}{E_1} = \frac{RQ + t_1 - (Q+Rt_1)t_2}{1 + RQt_1 - (R+Qt_1)t_2} \tag{23}$$

The features of each one of the equations obtained in this section, as well as the spectral response of the devices they describe, are shown in the results section.

III. Results and Discussion

A. Spectral response

In this section it is shown how the spectral response given by the equations obtained in the previous section does agree with the response expected by the coupled oscillators theory presented in any undergraduate classical mechanics book [17], which allows one to make an analogy between optical coupled resonators systems and coupled mass-spring systems. It is also shown how the devices' symmetry and topology have an influence over their transmission spectrum.

The first transmission spectrum is the one from the device with two cavities (equation 16 and figure 6). To calculate its spectral response the following parameters were considered:

- $A_1 = A_2 = 0.95$
- $k_1 = 0.312$
- $neff_1 = neff_2 = 3.15$
- $L_1 = 150\mu m$ and $L_2 = 75\mu m$

Using these parameters ensures that the resonances of both cavities are on the same wavelength. This is a key condition to show the main characteristics of this PM topology.

The normalized power transmission is calculated by taking the transfer function and multiplying it by its complex conjugate. Doing these calculations for equation 16, considering input waves with variable wavelengths in a range between 1.562 μm and 1.567 μm, the following spectra are obtained for two different coupling strengths:

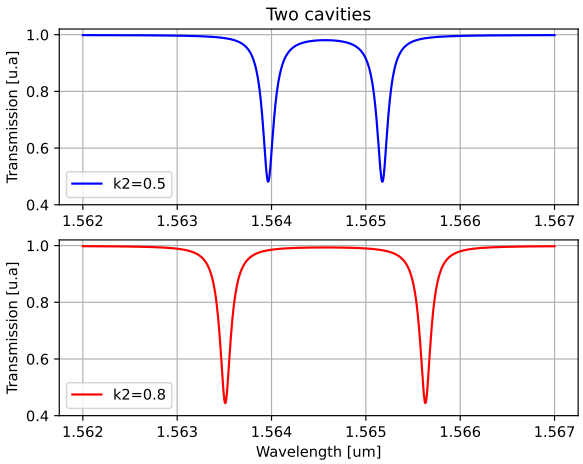

Fig. 9. **Two transmission spectra for different values of coupling between the two cavities. The top image shows the resultant spectrum for a coupling coefficient $K_2 = 0.5$, while the bottom image shows the transmission for $k_2 = 0.8$. From:** Author

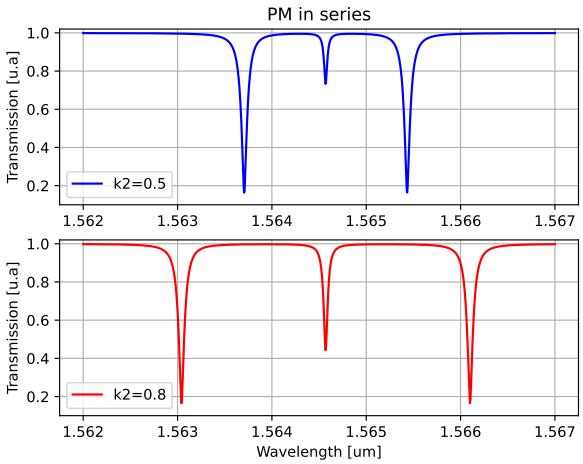

Fig. 10. **Two transmission spectra for different values of coupling between the bigger cavity and smaller cavities. The top image shows the resultant spectrum for a coupling coefficient $K_2 = k_3 = 0.5$, while the bottom image shows the transmission for $k_2 = k_3 = 0.8$. From:** Author

In the spectra shown in figure 9, it is possible to see two resonances. These two resonances appear because, even though the system has two cavities with the same resonance frequency, these cavities are coupled, and as in any system composed of coupled oscillators there is a change in the frequency of the resonant modes [17], this means that the resonances are "split" and the separation between the resultant resonances is governed by the coupling strength of the system, as can be seen on the figure 9. When the coupling factor is increased, the splitting of resonances also increases.

The next study is from the series device (represented in figure 7). For this device, the following parameters were considered, in which again, the resonant frequency of all cavities was the same.

- $A_1 = 0.95$ and $A_2 = A_3 = 0.99$
- $k_1 = 0.312$ and $k_2 = k_3$
- $neff_1 = neff_2 = neff_3 = 3.15$
- $L_1 = 150\mu m$ and $L_2 = L_3 = 75\mu m$

Considering the spectral range from 1.562 μm to 1.567 μm and two different coupling strengths, one for $k_2 = 0.3$ and the other for $k_2 = 0.8$, the spectra shown in figure 10 are obtained.

The same effect of resonance splitting is observed in figure 10, but in this case, the resonance frequency is split into three resonances, as was expected for a system composed of three coupled resonators. Again, as the coupling strength has increased the separation between the resonances and the extinction factor of the central resonance increases. The central resonance of this spectrum is called a quasi dark-state, and as it is shown on [10] the CMT method is not able to predict this resonant mode without using a correction.

The last study is the spectral analysis obtained by equation 22 (which refers to the parallel device, shown in figure 8), using the following parameters:

- $A_1 = 0.95$ and $A_2 = A_3 = 0.95$
- $k_1 = 0.312$ and $k_2 = 0.5$
- $neff_1 = neff_2 = 3.15$
- $L_1 = 150\mu m$ and $L_2 = L_3 = 75\mu m$

With the parameters shown above all three cavities of the PM has the same resonance frequency. Instead of considering two values for the coupling strength (k_2) in this case, it was considered two different values for the refractive index of one of the parallel cavities. Since they have the same length and coupling coefficient, these cavities become identical when the refractive index of the parallel cavities is the same, and then, the system has symmetry. This situation is shown in the top image of figure 11.

In the spectrum cited in the previous paragraph (top spectrum of figure11), it is seen just two resonances rather than three, which would be expected for a three-oscillator system as shown in figure 10. The lack of central resonance observed in the transmission spectrum is called a dark state, and this effect appears due to the system's symmetry. As the two parallel cavities have the same parameters, they have the same impact as they were just one cavity, which is equivalent to reducing the degrees of freedom of the system for an equivalent one composed of two resonators as the one shown in figure 6. It's possible to observe that this spectrum is the same present on the top image of figure 9.

When the symmetry of the system is broken, which was done in this case by adding a perturbation on the refractive index of one of the parallel cavities, the dark state is also broken, and a central resonance appears on the spectrum. It happens because in the case of a slight perturbation in one of the cavities they are not exactly equal as before, then they behave as two different cavities. In any case, the graph theory presented here adequately describes the spectral response for both situations.

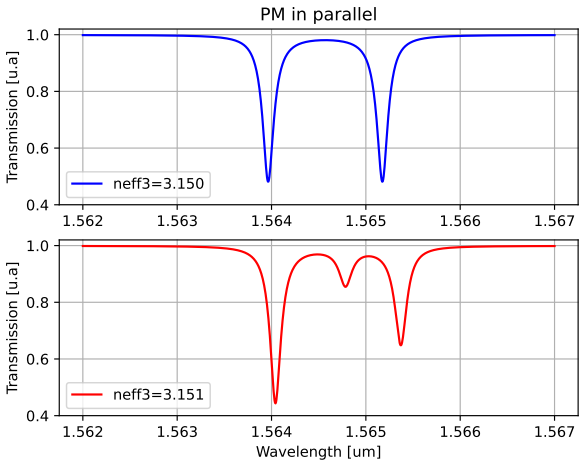

Fig. 11. **Two transmission spectra for different values for the refractive index of one of the smaller cavities. The top image shows the resultant spectrum for a refractive index of $neff_3 = 3.150$, while the bottom image shows the transmission considering $neff_3 = 3.151$. From:** Author

IV. Conclusion

This work showed how it is possible to model PMs in a practical and easy way using the graph method, which considers the coupling relations given by TMM. With the modeling tool shown here, it is possible to model complex photonic systems composed of many coupled resonators with the assistance of symbolic computation software, which will be in charge to calculate the matrix operations. This work also showed how the symmetry of coupled optical resonators system has an effect on the resultant spectra, being possible to tune between dark states and quasi-dark states by adding small perturbations to the coupled system.

References

[1] LUAN. E. et al. Silicon photonic biosensors using label-free detection. *Sensors*, 18:3519, 2018.

[2] BAREA. L. A. M. et al. Photonic molecules for application in silicon-on-insulator optical sensors. *Silicon Photonics XIII*, 10537, 2018.

[3] CHAN. J. et al. Laser cooling of a nanomechanical oscillator into its quantum ground state. *Nature*, 478:89–92, 2011.

[4] ZHANG. M. et al. Synchronization of micromechanical oscillators using light. *Physical Review Letters*, 109:233906, 2012.

[5] SIPSON. P. et al. Integrated silicon photonics for high-speed quantum key distribution. *Optica*, 4:172–177, 2016.

[6] PAESANI. S. et al. Experimental bayesian quantum phase estimation on a silicon photonic chip. *Physical Review Letters*, 118:100503, 2017.

[7] BARÊA L.A.M. Moléculas Fotônicas para aplicações em engenharia espectral e processamento de sinais ópticos., 2014. Tese (Doutorado) – Instituto de Física Gleb Wataghin, Universidade Estadual de Campinas, Campinas-SP, Brasil.

[8] M. ZHANG et al. Electronically programmable photonic molecule. *Nature Photonics*, 13:36–40, 2019.

[9] MORAS. ANDRÉ. L. et al. Integrated photonic platform for robust differential refractive index sensor. *IEEE Photonics Journal*, 12(5):1–10, 2020.

[10] MARIO C. M. M. SOUZA et al. Modeling quasi-dark states with temporal coupled-mode theory. *Opt. Express*, 24(17):18960–18972, Aug 2016.

[11] A. YARIV. Universal relations for coupling of optical power between microresonators and dielectric waveguides. *Electronics Letters*, 36:321 – 322, 03 2000.

[12] H.A. HAUS and W. HUANG. Coupled-mode theory. *Proceedings of the IEEE*, 79(10):1505–1518, 1991.

[13] WONJOO. SUH et. al. Temporal coupled-mode theory and the presence of non-orthogonal modes in lossless multimode cavities. *IEEE Journal of Quantum Electronics*, 40(10):1511–1518, 2004.

[14] REZENDE F.M.G. Projeto, caracterização e análise de microressonadores óticos acoplados em plataforma SOI, 2015. Tese (Mestrado) – Instituto de Física Gleb Wataghin, Universidade Estadual de Campinas, Campinas-SP, Brasil.

[15] ZIMMERMANN. H MASON. S. Electronic Circuits Signals and Systems., 1960. New York: Wiley. http://catalog.hathitrust.org/api/volumes/oclc/565172.html.

[16] BARÊA L.A.M. Desenvolvimento de Estruturas Monolíticas de Guias de Ondas Acoplados a Micro-Cavidades., 2010. Tese (Mestrado) – Instituto de Física Gleb Wataghin, Universidade Estadual de Campinas, Campinas-SP, Brasil.

[17] THORNTON. S. T MARION. J. B. Classical Dynamics of Particles and Systems., 1995. Fort Worth: Saunders College Pub.. http://catalog.hathitrust.org/api/volumes/oclc/565172.html.